Optimization of the integration of photovoltaic systems on buildings for self-consumption – Case study in France

Martin Thebault, Leon Gaillard

Highlights

Optimization of the integration of photovoltaic systems on buildings for self-consumption - Case study in France

Martin Thebault, Leon Gaillard

- Different objectives related to PV self-consumption are defined
- The optimization of PV integration according to these objectives is analyzed
- Roof and façades are considered
- A parametric study is carried out to study the influence of the sizes of the building and its energy consumption on the optimal PV integration

Optimization of the integration of photovoltaic systems on buildings for self-consumption - Case study in France

Martin Thebault[a], Leon Gaillard[a]

[a]*University Savoie Mont Blanc, LOCIE/FRESBE, F- 74944 Annecy-le-Vieux, France*

Abstract

The massive deployment of Photovoltaic (PV) energy in cities, which is expected in the coming years, brings new challenges when it comes to controlling power variations inherent to the impact of high PV penetration on the economy, energy exchanges and grid stability. In this perspective, self-consumption, which consists in consuming locally a part of the produced PV energy, allows to smooth the variations in the solar power production, and therefore reduce the stress on the grid. Among other strategies, self-consumption can be enhanced by the adequate use of all the surfaces of a building (roof and façades). In the present work, the optimization of the PV integration on the roof and façades of a building, is performed in order to optimize objectives related to self-consumption. These objectives are based on different aspects of self-consumption: minimizing the exchanges of energy with the grid, improving grid stability, or maximizing the economic profitability. The case of France will be considered. The influence of different parameters, namely, the load profile, the building consumption and height, on the optimal integration of PV will be investigated. It is shown that the optimal PV integration is drastically impacted by the studied parameters, and the goal of the optimization. Furthermore, integration on façades appears to be most of the time relevant in order to enhance self-consumption.

Keywords: photovoltaic integration, solar building, self-consumption, optimization, façade integration

1. Introduction

Repeated and constant calls to action leave no doubt as to the need for rapid and far-reaching responses to initiate and carry out a massive energy transition [1, 2].

Cities are directly responsible for about two-thirds of the world's final energy use, as well as 75% of global carbon dioxide (CO2) emissions. In addition, cities concentrate 55% of the world's population and 80% of the world's gross domestic product. Thus, the shift to renewable energy in cities is essential to decarbonize the global energy system [3]. Among the renewable energies, Photovolatic (PV) solar energy is particularly suited for urban environment. Indeed, cities represent areas with high energy consumption. In these areas, a lot of unused surfaces (roofs and façades) could be used for the harvesting of solar energy.

Power generation using PV technologies has experienced sustained and accelerated expansion since its commercial development a few decades ago. In 2019, accounted for 2.6% of the global electricity production and is expected to cover 25% of the world's electricity needs by 2050 [4]. It is also estimated that 40% of this energy will be produced from building integrated PV panels [4].

However, a high penetration rate of PV energy raises issues especially those of the intermittent and variable features of the solar resource and the management problems of the grid they may cause [5, 6, 7, 8]. One of these challenges concerns the excess of production of PV energy, which can cause reverse power flows. These can destabilize the stability of the electrical grid [5, 9, 7]. Sudden variations in the electrical power load, also called ramp rates, also represent an issue when high levels of PV penetration are reached [10].

To address these challenges, different strategies have been developed in order to limit and/or smoothen these variations. Among them, the use of storage and curtailment [11, 12], higher flexibility, or load shifting to limit overproduction [9], have proven relevant. Another way to reduce the impact on the grid is to inject less energy in it by consuming a part of the PV energy production locally [13, 11]. This is referred to as self-consumption, which is particularly adapted to urban environments where each building is a consumer as well as a potential producer of energy.

The two most common configurations for self-consumption are the on-grid and the off-grid configurations. The off-grid configuration consists in a building equipped with PV systems which is not connected to the grid. In this case, all the produced energy from the PV systems must be consumed by the building, either through direct use or by using storage. In Europe, the off-grid configuration corresponds to a small minority of the cases and has, by definition no impact on the electrical grid. The on-grid configuration is a building equipped with PV systems, which injects whole or a part of its PV production to the grid. This configuration represents the large majority of the cases, especially in urban environments.

Limiting reverse power flows and ramp rates are objectives at the scale of a region/territory. For that reason, the use of self-consumption to smoothen load variations on the grid is relevant for grid managers or policymakers whose goal is to accelerate energy transition on their territory. However, building owners are probably less aware of these challenges and will consider self-consumption as a way to increase the economic profitability of a PV system [13, 14, 15]. For that reason, enhancing self-consumption can have different interpretations depending on the objective that is pursued.

The vast majority of studies on the impact of urban PV on the grid only considered rooftop PV systems, mostly because of their maturity, their easy integration and their low cost. However, the strong decrease in prices of PV systems, which is likely to continue in the coming years [16, 17], allows to consider the integration of PV on vertical façades as economically viable. This opens engaging perspectives in urban environments where the available area on façades is sometimes much larger than that on roofs [18, 19].

One of the specificity of PV on façades is to have different profiles of power production different from those of PV on the roof. Indeed, east and west oriented PV panels have their peak production shifted compared to a roof-integrated PV. This allows them to produce more energy in the morning and evening [20, 19]. Panels installed on the southern façades are relatively less affected by seasonal variations [21]. Therefore, the optimization of PV integration, including all façades, appears as an interesting strategy to enhance self-consumption.

Optimization of the harvesting of solar energy has mainly been conducted by optimizing urban design in order to maximize the collection of solar energy (see e.g. Kämpf et al. [22], Bizjak et al. [23]). In recent years, particular focus has been on optimizing the matching between energy consumption and solar production (see e.g. Widén et al. [24], Natanian et al. [25], Waibel et al. [26]). These studies optimized the whole urban design *i.e.* the shapes and orientations of buildings. However, building new district is costly and time-consuming. It is therefore very likely that most of the PV systems will be installed on existing buildings.

Some studies have recently focused on the optimal integration of PV on the roofs and façades of existing buildings. Brito et al. [27] showed that under Mediterranean latitude, the power production of the façades was better matching the building load, therefore reducing the net energy load on the grid. Freitas et al. [28] conducted a study on the optimization of PV production on roofs and façades on the scale of districts and showed the importance of PV integration on façades, especially for the reduction of the ramp-rates and increase in self-consumption. However, Freitas et al. [28] showed that, for a same installed capacity, the PV integration varied drastically if surfaces that are the most irradiated are used first, or if the surfaces are selected in order to maximize the self-consumption rate.

All these studies focused on the district scale and conducted the optimization by considering the entire façade of a building. However, because of technical, energetic or economic constraints, it often occurs that only a certain part of the roof area is suitable for PV integration [29, 30]. As a consequence, integrating PV system on the entire façade of a building, when it is possible, is likely not to be considered optimal, depending of the pursued objective.

The aim of the present work is to investigate the optimal integration of PV on building surfaces considering different self-consumption objectives. The first objective is the maximization of the load match. In this case, the PV systems are integrated so that the power production of the PV matches as closely as possible the building load. This results in a reduction of the energy interactions between the grid and the building equipped with PV. The improvement of the load match has been used in several studies (see e.g. [24, 25]). The second objective aims to reduce the occurrence and intensity of the ramp-rates in the power exchanges between the building equipped with PV and the grid. The third objective is economic and consists in maximizing the profitability of the system.

The main contributions of the present work are:

- Defining different metrics related to self-consumption and presenting the associated optimal integration of PV systems,
- Investigating the influence of the size of the building and its consumption on the optimal integration of PV systems,
- Studying the role of the façade integration of PV panels in order to enhance self-consumption.

Optimal PV configuration is highly dependent on the local context. Indeed, differences in latitude and longitude have a significant impact on the integration on the façade. Furthermore, the local economic context also has a strong influence on the optimization of the PV integration. For that reason the present work will be illustrated in the French context.

2. Methodology

2.1. Geometry and usable surfaces

A single building with a flat roof will be considered here. This building will have a footprint area equal to the roof surface area of $S_r = 10 \times 10\ m^2$. For the sake of clarity we also neglect the wall width so that S_r is also equal to the area of a floor S_f. The building is composed of N_f floors, each floor being 3 m high. Three of these buildings are illustrated in Figure 1. They have respectively N_f=2, 5 and 10 floors and will be further referred as 'low-rise' 'mid-rise' and 'high-rise' buildings. The surfaces are aligned with the cardinal directions. Note that, unlike what is

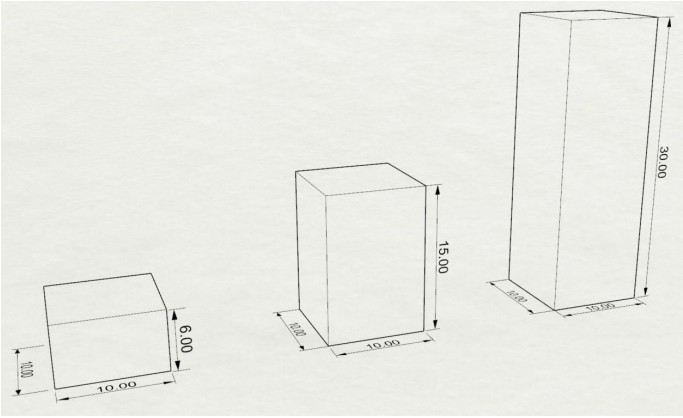

Figure 1: Geometry of the 'low-rise', 'mid-rise' and 'high-rise' buildings

seen in Figure 1, these building are considered to stand alone, without any possible shading from other buildings.

The roof as well as the east, west and south façades will be considered in the present work. The north façade is disregarded as it is shaded most of the time. On the roof, the PV systems are tilted at an angle of 30°, facing the south, and cannot occupy more than 70% of the surface to avoid self-shading [31]. For a building of N_f floors, the total living area corresponds to $N_f \times S_f$. According to the French building standards, the glazed surface on the façade must cover at least $1/6$ of the total living area. Now, considering that the glazed surfaces are equally shared between the four vertical façades, on each façade the usable surface is reduced by a quarter of the total glazed area. Therefore, the usable surface area of each façade is equal to

$$S_{u,i} = S_{T,i} - \frac{1}{4} \times \frac{N_f \times S_f}{6}, \tag{1}$$

Where $S(m^2)$ refers to a surface area, the subscripts T and u respectively refers to the total and the usable surface area of a façade. The subscript $i = e, w, s$ refers to the east, west and south façades.

2.2. Production and consumption of the building

In what follows, P (kW) and L (kW) will correspond respectively to the power production and the power consumption (load) of the building. It is also considered here that the energy produced by the PV system is used for the building energy needs. Only when the PV production exceeds the building energy needs, the excess of production is sold to the grid. Therefore the self-consumed energy during a period T is defined by

$$E_{sc} = \int_T min(P(t), L(t))\mathrm{d}t. \tag{2}$$

The energy sold to the grid, which corresponds to an excess of production that cannot be consumed locally, is defined by

$$E_e = \int_T max\left(P(t) - L(t), 0\right)\mathrm{d}t. \tag{3}$$

In order to quantify power and energy exchanges between the building equipped with PV systems and the grid, the residual load $L_r(t)$ (sometimes called residual or net load) is introduced. It is defined as the difference between load and production *i.e.*.

$$L_r(t) = L(t) - P(t). \tag{4}$$

In the present problem, it is considered that there are no shades from the surroundings so that the received solar irradiation is uniform on each surface. Thus if we consider $p_k(t)$ (kW/m^2) the PV production per surface area with $k \in \{r, e, w, s\}$, the building's PV power production can be expressed as

$$P(t) = \sum_{i=r,e,w,s} S_{PV,i} \times p_i(t) \tag{5}$$

where the PV index indicates the surface covered by the PV panels. For $i \in \{r, e, w, s\}$, we have $0 \leq S_{PV,i} \leq S_{u,i}$. Note that in equation 5, we neglect non-linear phenomena that may impact the total PV production. Indeed, several factors may impact the PV production, the temperature of the PV systems being one of the best known and most influential [32], [33]. However, here, the fact that the building is considered to stand-alone, without any surrounding buildings, drastically reduce the urban heat island effect. Moreover, the loss of performance would correspond to some % during the hottest day [32], which would not significantly change the results of the present work. As a matter of fact, most of the studies that were mentioned in the introduction neglect the influence of temperature on the PV production.

2.3. Self-consumption and optimization objectives

One of the main goals of the global PV deployment is to drastically increase the share of PV production in the energy mix. To achieve this objective at the scale of building, all possible available areas (roof and façades) should obviously be covered by PV panels. However, this objective is different from the objective related to self-consumption, in which a certain balance between production and consumption should be considered.

First of all, we define the classical metrics of self-consumption [13] which are the rate of self-consumption, τ_{sc}, and the rate of self-sufficiency τ_{ss}. The self-consumption rate τ_{sc} is defined as the share of the total PV production that is consumed by the building. The self-sufficiency rate τ_{ss} is defined as the share of total building energy demand that is being supplied by the PV systems *i.e.*:

$$\tau_{sc} = \int_T \frac{min(P(t), L(t))}{P(t)}, \quad \tau_{ss} = \int_T \frac{min(P(t), L(t))}{L(t)}, \tag{6}$$

T being the considered time period, in this case a year.

These two metrics cannot be considered here as objectives in mono-objective optimization. Indeed, a self-consumption rate of 1 is always achievable if the PV energy production is low enough in comparison with the energy needs of the building. Conversely, in order to maximize self-sufficiency, it is sufficient to maximize PV production. However, as mentioned in the introduction, self-consumption allow to attenuate some of the interactions with the grid, and neither the maximization of τ_{sc} nor this of τ_{ss} can guarantee this.

The optimization of PV integration will therefore be done according to other objectives. The first one corresponds to a minimization of energy exchanges with the grid. The second one is based on the minimization of the reduced load variations, and the third one is an economic objective, based on a maximization of the NPV (Net Present Value).

2.3.1. Objective 1: Minimization of the energy exchange with the grid

The first optimization objective consists in minimizing energy exchanges between the building and the grid. This corresponds to minimizing

$$E_{grid} = \int_T |L_r(t)|dt. \tag{7}$$

This objective allows to obtain the best matching between the PV production and load of the building. This is particularly interesting in order to limit the oversupply or undersupply of solar energy on the grid which would be induced by a massive increase in decentralized PV systems, as mentioned in the introduction.

In order to assess the efficiency of the integration, an Energy Exchange (EE) indicator will be defined as

$$\tau_{EE} = \frac{E_{grid}}{\int_T |L(t)|dt}. \tag{8}$$

This indicator is defined as the amount of energy exchanged with the grid by a building equipped with PV panels, divided by the amount of energy exchanged by the same building but without any PV panels. In other words, this indicator quantifies to which extent the PV panels reduces or increases the stress on the grid compared to the same building without PV. When $\tau_{EE} < 1$, the PV integration reduces the energy interactions with the grid, whereas when $\tau_{EE} > 1$, the PV integration increases energy exchanges with the grid.

2.3.2. Objective 2: Minimization of the reduced load variations

The second objective is minimizing the ramp rates (RR). Ramp rates are sudden variations of power on the grid. In the case of a building with PV panels, ramp rates correspond to variations in the reduced load L_r. The RR is defined here as

$$RR(t) = \frac{L_r(t + \Delta t) - L_r(t)}{\Delta t} \tag{9}$$

and the objective will be to minimize the standard deviation of the RR, $\sigma(RR)$.

Similarly to objective 1, an indicator is defined to assess the improvement in the RR attenuations. It is defined as

$$\tau_{RR} = \frac{\sigma(RR)}{\sigma\left(\frac{L(t+\Delta t)-L(t)}{\Delta t}\right)}. \tag{10}$$

A value of τ_{RR} smaller than 1 means that the variations in the ramp rates decrease compared to the case in which the same building does not have PV installation.

2.3.3. Objective 3: Maximization of the economic benefits

There are several metrics to quantify the economic benefits from PV systems [14, 34]. Among them, the Net Present Value, NPV is the most widely [14]. It is defined as

$$NPV = B_L - C_L \tag{11}$$

where B_L and C_L respectively correspond to benefits and costs of the system during its lifetime $L = 30$ years [14].

Benefits are calculated as [14]

$$B_L = S_0 + \sum_{k=1}^{L} \frac{E_{sc} p_r + E_e p_w}{(1+d)^k}, \tag{12}$$

where d is the discount rate, evaluated by Sommerfeldt and Madani [14] at 3%. S_0 corresponds to subsidies, E_{sc} is the self-consumed energy (defined in eq.2) and therefore $E_{sc} p_r$ corresponds to savings made by deferring purchases to the grid at the retail price p_r. E_e corresponds to the excess production of energy (defined in aq.3), sold to the market at the wholesale price p_w.

Costs are calculated as

$$C_L = I_0 + \sum_{k=1}^{L} \frac{OM_k}{(1+d)^k}. \tag{13}$$

The yearly operations and maintenance costs at year k (OM_k)are evaluated at a fixed cost of 1% of the investment I_0 [14], the latter being the sum of the investment in the panels installed on the roof I_R and on the façades I_F.

2.4. Case study: French part of the Great Geneva

The present work is conducted as part of a French-Swiss project in the cross-border region of the Great Geneva.The case of a building on the French part of the Great Geneva will be studied here.

2.4.1. Climate and weather

Great Geneva has a continental weather and a latitude of 46.2°. Continental climate appears in more than half of Europe and large regions in Asia and North America. Moreover, the latitude of these regions remains close to those of Geneva. For these reasons, some the results of the present study can be generalized for a much wider region than only the Great-Geneva region.

The weather conditions for a standard year (.epw file) were taken from Geneva weather station, located at Geneva airport. This weather station is located at the French-Swiss border so that the weather file can be used for French or Swiss conditions.

2.4.2. PV production and building load

The PV production throughout the year was simulated with the help of EnergyPlus software for the estimation of incident solar radiation on each outdoor surface.

For the load curve, real consumption profile were used. Referred to as $l(t)$, they correspond to a non-dimensional aggregation of the consumption profiles in French Geneva. Therefore, the consumption of the building is defined here as

$$L(t) = K \times A_T \times l(t) \tag{14}$$

where K ($kWh/(m^2.y)$) is the annual energy consumption density of the building and $A_T = S_r \times N_f$ is the total living area. The time step for both the PV production and the building energy consumption is $\Delta t = 10$ min.

Except when explicitly mentioned in section(3.2), in the rest of the manuscript the focus will be on the tertiary building load profile. One of the main reasons is that tertiary building are particularly interesting for PV self-consumption as the energy consumed by these building is higher during daytime, when there is PV production.

2.4.3. *Economical data*

In order to calculate the economic parameters defined in section 2.3.3, p_r is taken at 15 cts/kWh, the French mean price in 2020. p_w and S_0 depend on the total installed capacity as indicated in Table 1.

Total PV capacity (kWp)	[0-3]	]3-9]	]9-36]	]36-100]	> 100
p_w in cts/kWh	10	10	6	6	0
S_0 in €/kWp	390	290	180	90	0

Table 1: Subsidies and retail prices for self-consumption in France in September 2020

In the French context, S_0 and p_w only depends on the installation size and the date the PV installation is connected to the grid (here prices are for April 2020). A contract with the energy provider prevents p_w to change over the lifetime of the system. Nevertheless, it is very likely for the price of energy, and therefore p_r to change in the coming years. It is extremely difficult to predict but it is very likely that this price will increase which should make self-consumption more profitable

I_R can be easely estimated from the French market prices [35] as was reported in Figure 2. To approximate these data, two power-law interpolation curves were used between 5 and 100 kWp and between 100 and 800 kWp respectively. As for I_F, it is much more difficult to estimate because of the lack of economic data about façades. In the present work, this cost is regarded as following a law similar to that of I_R multiplied by a factor of 1.5, which is coherent with previously used economic estimations [16]

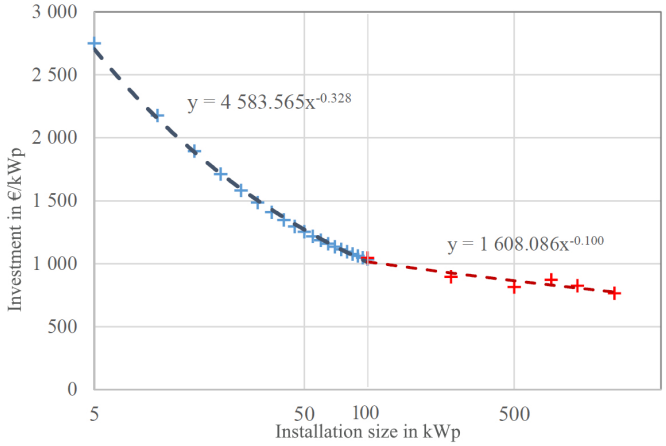

Figure 2: Investment costs for roof mounted PV system I_R as a function of the total installed capacity. Symbols represents average market prices and dotted line represent interpolation of these data. Two interpolation curves were used, a power law in the range [5,100] and a linear interpolation for installed capacity greater than 100 kWp.

2.5. *Optimization functions and variables*

The three objectives that needs to be optimized are:

- Obj.1 - E_{grid} (eq.7),

- Obj.2 - $\sigma(RR)$ (eq.9),
- Obj.3 - the NPV (eq.11).

In these optimization problems, the areas that PV systems cover on each of the surfaces are optimized. In other words, the variables of the optimization problems are $S_{PV,i}, i \in \{r, e, w, s\}$. The variables are therefore bounded by the absence of PV panels and by $S_{u,i}$, $i \in \{r, e, w, s\}$, the maximum usable areas on each surface. In Obj.1, E_{grid} depends on $P(t)$ which is directly proportional to $S_{PV,i}$ (see eq.5). From eq.9 it is also straightforward how $\sigma(RR)$ depends on $S_{PV,i}$. Finally, regarding Obj.3, the NPV depends on B_L which depends on E_{sc} and E_e, both dependent on $P(t)$ and therefore on $S_{PV,i}$. Furthermore, as was presented in section 2.4.3, the economic parameters S_0, I_0, p_w and OM_k also depends on the total size of the PV installation and therefore on $S_{PV,i}$.

Therefore it appears that for each objective $q = 1, 2, 3$ the optimization problem can be simply written as

$$\min_{S_{PV,i}} \left\{ f_q(S_{PV,i}), S_{PV,i} \in [0, S_{u,i}] \right\}, i \in \{r, e, w, s\}. \tag{15}$$

The objective functions f_1 and f_2 are respectively E_{grid} and $\sigma(RR)$ whereas $f_3 = -NPV$. Indeed, the minimization of f_3 corresponds to the maximization of NPV. In order to minimize the objective functions, the 'fmincon' optimization solver from the Matlab environment is used [36]. 'fmincon' algorithm uses gradient based methods and can be used with continuous multi-variable objective function.

It can be noted that I_R, I_F, p_w and S_0, are non-continuous piecewise defined functions, which make the direct use of the 'fmincon' optimization solver impossible. In that case, the optimization is made on each sub-interval on which the objective function is continuous. Here it corresponds to the intervals defined by the PV total installed capacity ranging in [0,3],]3,9],]9,36],]36,100] and]100,+∞]. It therefore provides five local minima. Then the global minimum is simply taken as the minimum of the local minima.

Finally, the objective functions are minimized considering the load and production profile of an entire year.

3. Results

The next section presents the results of the optimization according to these various parameters. First the influence of the objective on the optimal integration is presented. Then the influence of the building load profiles is looked at. Finally, a parametric study of the impact size and energy consumption of the building is presented.

3.1. Optimal PV integration strategies depending on the objective

Different strategies, all linked to self-consumption, may lead to different PV integrations. This is illustrated in Figure 3, where the optimal integration for each of the objectives is presented. In this figure, all the considered façades and the roofs are shown in unfolded view. The colour shades indicate the percentage of the usable surface that is covered by PV panels.

It first appears that the optimal PV integrations are fundamentally different depending on the objective. In the case of the low-rise building, Obj.1 favors vertical façades and the roof is not entirely equipped whereas the opposite integration is obtained for the third objective. This

Figure 3: Unfolded view of the roof, east, south and west façades of the buildings under study. From top to bottom: low-rise, mid-rise and high-rise buildings. From left to right: Obj.1 , Obj.2 and Obj. 3. The colours indicate the PV coverage rate of the surfaces (Red: no panels on the surface. Dark green: the entire available surface is used). Case of an annual surface consumption of K =50 kWh/(m^2.y).

derives from the economy of scale and the subsidy scheme. Indeed, for the low-rise and mid-rise buildings, the inclusion of PV on the vertical façades is not profitable whereas it becomes profitable for the high-rise building. However, the west and east façades are not fully covered. This is because the installed capacity reaches 100 kWp, a threshold after no more subsidies are granted (see table 1). The optimal integration according to Obj. 2 consists in a small coverage of the east and west façades whereas the roof is entirely covered only for the highest building.

In order to better understand the results of the optimizations, it is possible to plot, on the same graph, the PV production for each façade and the building load. This was done in Figure 4 for the low-rise building with an annual consumption of $K = 50kWh/(m^2.y)$. The low-rise building is chosen here because the optimal integration have strong differences. In this figure, the production of each façade P_k, the total PV production P and the building L are plotted on the same chart. To better visualize the load match during the sunny hours, the 'lack' of energy - when the PV production is lower than the building load - has been coloured in blue, and the 'excess' - when total PV production exceeds the building load - have been coloured in orange.

It can be seen that in the case of Obj.1, east and west façades are almost fully covered, which produces a 'double hump' in the production profile. This characteristic makes it possible to better match the load of the building which also has a 'double hump'. In the case of Obj. 3, the PV

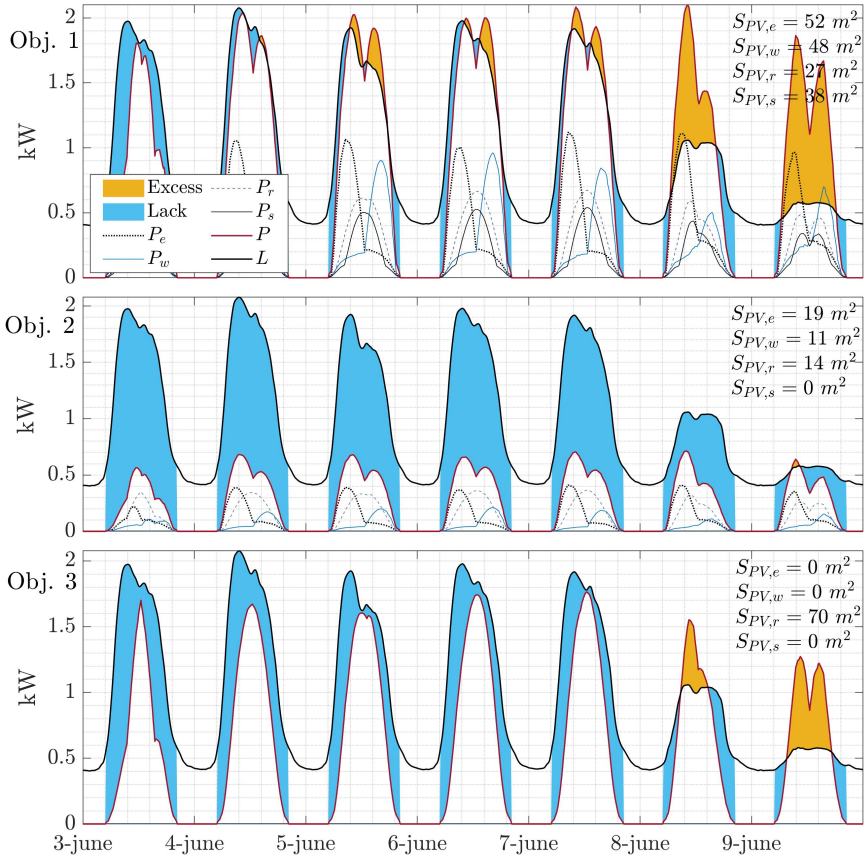

Figure 4: Production (red) and load (black) curves for the low-rise building and for the three optimal PV integration (Obj. 1 to 3). The blue and orange areas correspond to deficits and excesses of production compared to consumption. The production curves for each façade are also plotted, but only visible for objectives 1 and 2 (for objective 3 the total production is equal to that of the roof, the others being zero).

production has the classic bell shape of PV production and covers a lot of energy needs in the selected week. Finally, with Obj. 2, energy production is low compared to consumption. The explanation is that here, the PV integration guarantees that the production ramps, that mainly occur in the early morning and at the end of the day, correspond to the ramps in the building load.

3.2. Influence of the load profile

Another factor that may influence the optimal integration of PV is the load profiles of the building. Indeed, the load profile shape is a key variable in the calculation of the three objective functions.

In Figure 5, the load and consumption curves of the low-rise building are plotted for a typical week of June, for three different load profiles and integration strategies. For Obj.1, the optimal PV configuration favors the vertical east and west surfaces. The south surface is also favored compared to the roof which is almost not used in the case of the residential load. This is because,

under the considered latitude, the PV production of the southern façade has less seasonal variations than that of roof. Given that the building load has low seasonal variations, it is better to reduce seasonal variations in the PV production by using the south façade.

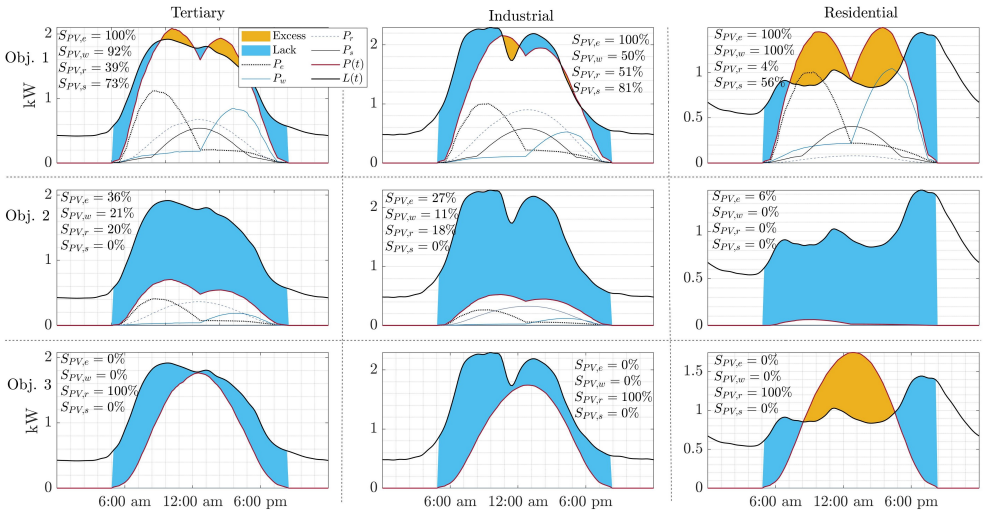

Figure 5: Production (red) and load (black) curves for the low-rise building. The production curves for each façade are also plotted. The blue and orange areas correspond to deficits and excesses of production compared to consumption. Typical weekday in June. From top to bottom : Obj. 1 to 3. From left to right: Tertiary, Industrial and Residential load profiles.

The optimal configurations, according to Obj.2, are similar for the industrial and tertiary loads. In these cases, there is a low coverage rate of the roof, west and east façades and no use of the southern façade. However, for the residential load, almost no PV should be integrated. The reason is that the residential load have no ramps that coincide with the PV production and therefore it is not possible to reduce the ramp rates in the reduced load. Finally, for Obj.3, the optimal configuration is the same for all the load profiles, the roof being entirely covered and the façades unused.

To sum up, for the considered building (low-rise, $K = 50kWh/(m^2.y)$), the load profile of the building has less influence on the optimal PV configuration than the optimization objective. Whereas façades appear to be better in order to reduce energy exchanges with the grid (Obj. 1), they are not interesting in order to reach maximum profitability.

It is important to note that the three load profiles that have been used here correspond to aggregation of a wide range of loads. Despite the fact that they are representative of the tertiary, industrial and residential load profiles, there is in fact more diversity in the shapes of the load profile and consequently, in the corresponding optimal PV integrations.

3.3. Parametric Study

In order to keep investigating the optimal PV configurations, it is necessary to assess the influence of fundamental building parameters which are their sizes and their consumption. In the present case, to modify the building size, the number of floors N_f will be changed. The energy consumption of the building will be changed by varying the electrical consumption density K in

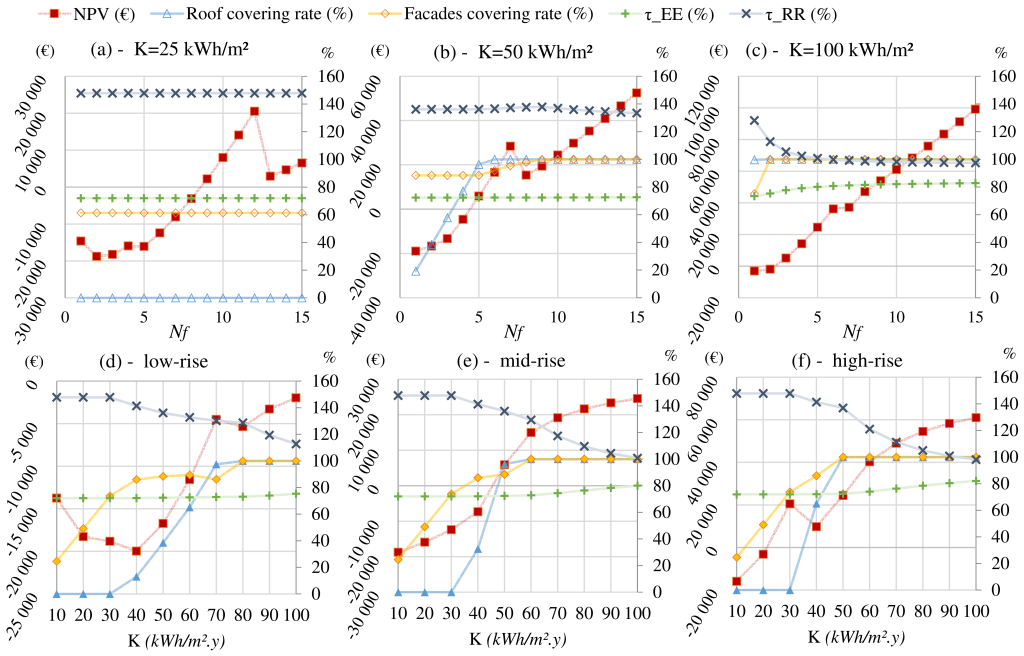

Figure 6: Optimal configuration according to Obj. 1: Minimizing the energy exchanges with the grid. For each x-value, the PV integration is optimized according to Obj.1. Evolution of the roof coverage (light blue triangle) and the façades coverage (orange diamond). They are expressed in % of the total usable surface, and their values is read on the right vertical axis. The three optimization indicators are also indicated: The NPV values (in €) can be read on the left vertical axis whereas the values of the energy exchange indicator τ_{EE} and the ramp rate indicator τ_{RR} can be read in % on the right axis . (a) K=25 $kWh/m^2/y$, (b) K=50 $kWh/m^2/y$, (c) K=100 $kWh/m^2/y$, (d) low-rise building, (e) mid-rise building, (f) high-rise building.

($kWh/(m^2.y)$). Note that, as was mentioned in section 2.4.2, in the remaining of the paper the tertiary building load will be used.

The parametric studies will be conducted for each parameter independently so that when N_f varies, K remain constant and inversely.

Different consumption densities of electrical energy will be considered here, $K = 25, 50$ and $100kWh/(m^2.y)$. $K = 50kWh/(m^2.y)$ corresponds to the consumption of a new efficient building according to French regulation and only using electrical energy. $K = 25kWh/(m^2.y)$ could correspond to a building that is using electrical energy in addition to another source of energy.

In the following sections, the influence of these parameters will be investigated for each of the optimization objectives.

3.3.1. Parametric study - Obj.1

A parametric study of the influence of the height of the building and its density of energy consumption on the optimal PV configuration is presented for Obj.1 in Figure 6. In this figure, six graphs are presented. On each graph, the NPV is read on the left vertical axis while the

energy exchange indicator τ_{EE} and the ramp rate indicator τ_{RR} can be read in % on the right axis. The coverage rate of roofs and façades, defined as the percentage of the usable surface covered, can also be read (in %) on the right axis.

In Figure 6 (a), (b) and (c), the building height evolved by changing the number of floors (N_f) while keeping the energy consumption density constant, respectively (a) K=25, (b) K=50 and (c) K=100 $kWh/m^2/y$. As was presented in section 2.1, one floor is 3 m high. Moreover, as the building gets higher, the livable surface also increases and with it the total energy consumed.

It first appears that the role of PV on surface is predominant here. Indeed, for each case, façades are covered in priority for smaller buildings or buildings with low energy consumption density K. However, as the size increases, both roofs and façades are used at their full potential (100% covering rate). The only exception is for building K=25 $kWh/m^2/y$ for which only façades are used, regardless of the building size.

Regarding the energy exchange indicator τ_{EE}, the one which is optimized here, it appears that its values remain relatively constant through the whole parametric study with percentage around 70% for low-mid values of K and N_f and values around 80% for higher buildings with high consumption densities.

In other words, it means that here, the PV configuration reduces the energy exchanges of a building with the grid by up to 30%.

It should also be noted that the NPV is negative for the small values of K and N_f meaning that the PV systems are not economically profitable in these cases. The peak that can be observed in the NPV in graphs (a), (b), (d) and (f) are due to the subsidies scheme (section 2.4.3), that is decreased as the total capacity increases and stops above 100 kWp of PV capacity installed.

Finally, the ramp rate indicator τ_{RR} has relatively high values around 150% except for high-rise buildings or buildings with high consumption for which the value drops to nearly 100%. This means that, when the configuration is optimum according to Obj. 1, the occurrence and intensity of the ramp rates significantly increases compared to a building without PV panels.

It can also be noted that except for the low-rise building in (a), the roof and façades reach their maximum capacity for high values of K and N_f. This means that, in these cases, the optimum configuration also corresponds to the maximum PV production.

3.3.2. Parametric study - Obj.2

Figure 7 is similar to Figure 6 except that this time, the PV integration is optimal according to Obj.2, which is the minimization of the ramp rates variations.

From this parametric study, it appears that the façades and roof covering rate varies almost linearly with the energy consumption density. The maximum PV capacity of the building is never reached in these cases. From the linear trends in (d) (e) and (f), we could expect the full covering of the façade to be reached at once, but this would occur for buildings with much higher energy consumption density.

Regarding the ramp rate indicator τ_{RR}, optimized here, its value remains equal to 91%, independently on the building size and consumption. Interestingly enough, the energy exchange indicator τ_{EE} is also constant with a value of 90%. This means that for any of the size or consumption level investigated here, there is a PV configuration, which reduces the ramp rate variations of the building equipped with PV by up to 9% while including the energy exchanges by nearly 10%.

However, it can be seen on the NPV evolution that, the PV configuration is only profitable for the high energy consumption density (c) or the high-rise building (f).

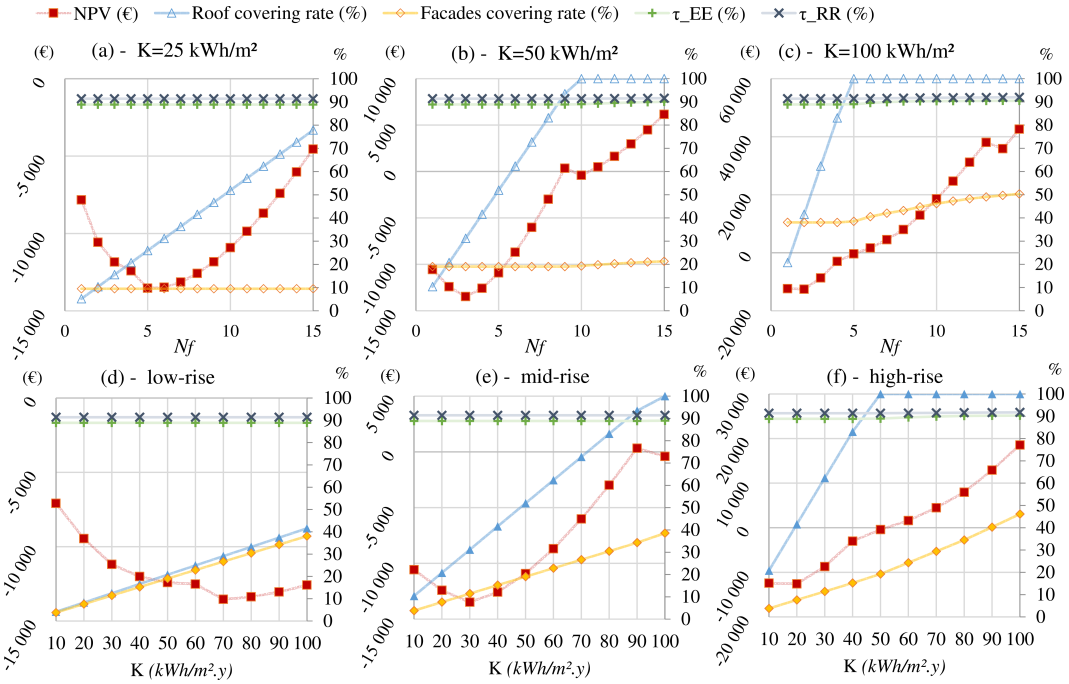

Figure 7: Similar as in Fig.6, (a) K=25 $kWh/m^2/y$, (b) K=50 $kWh/m^2/y$, (c) K=100 $kWh/m^2/y$, (d) low-rise building, (e) mid-rise building, (f) high-rise building, for each x-value, the PV integration is optimized according to Obj.2 (RR)

3.3.3. Parametric study - Obj.3

Figure 8 is similar to Figure 6 except that this time the PV integration is optimal according to Obj.3, maximizing the NPV.

In this case, the roof is covered, almost at its full capacity even for the lowest building height and consumption. Then, as soon as the building is high enough for the vertical surfaces to reach a PV capacity of 100 kWp, façades start to be covered. It is very interesting to note in (b), (c) and (e) that the façade coverage jumps from 0% to 100% at once. This implies very high sensitivity of the optimal façade coverage rate to the building parameters. In each case, the NPV increases with the size of the building and the its consumption density. However, in (a) and (b), it can be seen that the NPV reaches a plateau which stops as soon as façade integration becomes profitable enough to increase the NPV.

Here, the general trend is opposite to that observed for Obj.1. Indeed, in this case, roof are first equipped up to their full potential for low-mid values of N_f and K, and then the façades are covered. This could be expected, given that façade integration is more expensive in terms of initial investment, and globally less productive in terms of energy production. However, it should be noted that for highest values of N_f and K, the roofs and façades are fully covered. This was also the case for the optimal configuration according to Obj.1 (see section 3.3.1). In other words, for high values of N_f and K, the covering the entire surfaces with PV corresponds to the optimal configuration for both Obj. 1 and Obj. 3.

Finally, here, the energy exchange indicator τ_{EE} remains in the range of 80% to 100%, which means that all the optimal configurations according to Obj. 3 are also beneficial when considering

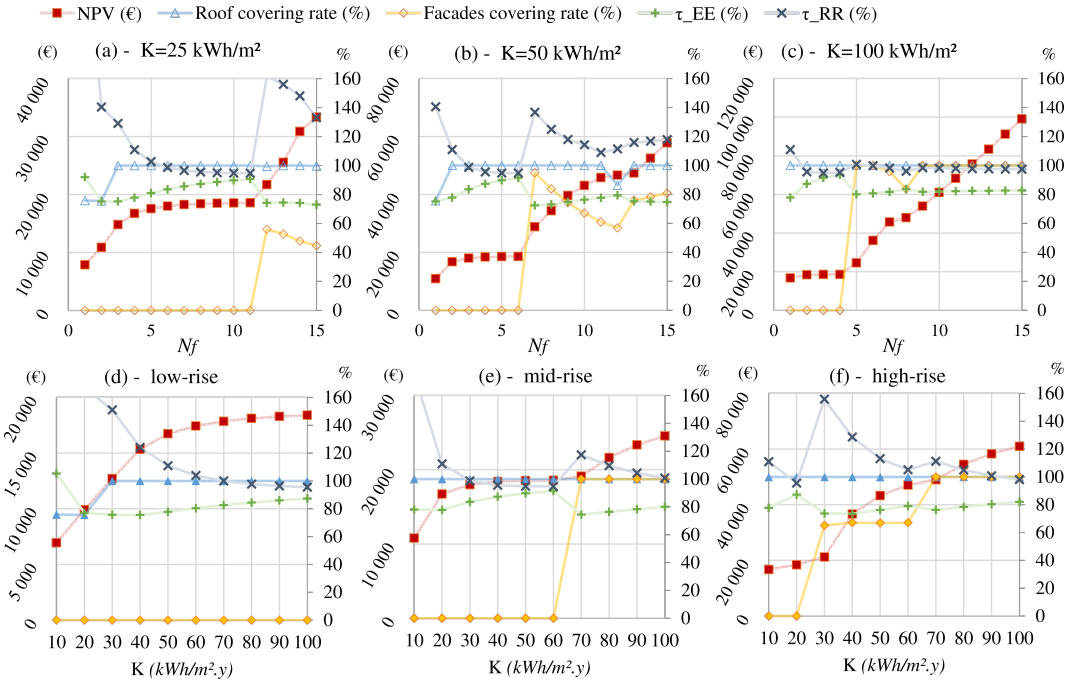

Figure 8: Similar as in Fig.8, (a) K=25 $kWh/m^2/y$, (b) K=50 $kWh/m^2/y$, (c) K=100 $kWh/m^2/y$, (d) low-rise building, (e) mid-rise building, (f) high-rise building, for each x-value, the PV integration is optimized according to Obj.3 (NPV)

the energy exchanges with grid.

4. Discussion and conclusion

In the present paper, optimization of the integration of PV on the roofs and façades of buildings is achieved based on different objectives related to self-consumption strategies. The first objective aims to minimize the energy exchanges with the grid. The second aims to minimize the reduced-load variations, also called ramp-rates (RR). The third objective is economic and corresponds to a maximization of Net Present Value (NPV). The case of France is investigated, and meteorological as well as economic inputs from France are considered.

It appears that most of the time, different self-consumption goals lead to different optimal PV configurations. Indeed, for low and mid-rise buildings or buildings with low or medium electrical energy consumption, the optimal configurations according to Obj.1 prioritize the uses of the façades whereas roofs are prioritized when Obj. 3 is pursued. However, for high-rise buildings or buildings with high energy consumption, the differences vanish for Obj.1 and 3, once the full coverage capacity of the roof and the façade is reached. In other words, for these buildings the PV configuration minimizes energy exchanges with the grid while maximizing profitability.

When the power fluctuations are minimized (Obj.2), the surfaces of the buildings are most of the time only partially covered, the maximum covering rate being reached for the highest buildings and the highest energy consumption density.

The main observations and conclusions from the present works are:

- Different objectives linked to self-consumption lead to different PV configurations especially for low and mid-rise buildings with low energy consumption levels.
- The use of all the surface of the building (roof and façades) is crucial in order to better integrate solar energy. Façades are the most relevant in order to minimize energy exchanges with the grid, but they also become economically profitable for higher rise or more energy-consuming buildings.
- At the scale of a single building, minimizing the RR (Obj.2) leads to a rather low coverage of the roof and façades compared to other objectives.
- Optimal PV integration can reduce the energy exchanges with the grid of a building equipped with PV system by up to 30%.
- An adequate PV integration can reduce the load variation of a building equipped with PV by up to 9%.

From these results, several policy recommendations can be made. First of all, self-consumption has several co-benefits, which are economic as well as energetic (e.g., reduced grid energy consumption and power variations). Therefore, policies promoting self-consumption must be pursued. The current economic context and pricing schemes render the use of façades for PV energy production not economically profitable for small scale installations. However, the results of the present work demonstrate that the use of facades, even for small buildings, is significantly beneficial to the reduction of energy stress on the grid. It is also very likely that this 'profitability loss' is only a matter of scale. Indeed, the use of façades is likely to be not the most profitable solution for the owners of small buildings. However, considering a wider scale (regional/national), the use of façades will decrease the stress on the energy grid which, at last, will corresponds to energetic and economic benefits for the grid manager (who is a public actor in France). It will also allow a wider integration of renewable energy. Therefore, the subsidies and pricing schemes could evolve in order could be tailored to favor the use of the façades.

Acknowledgements

Authors would like to thanks the program INTERREG V Suisse-France for providing financial support to conduct this study in the framework of the project G2 Solar which aims at extending the solar cadaster to the Greater Geneva and intensify energy solar production at this level. This work has been supported by the French National Research Agency, through Investments for Future Program (ref. ANR-18-EURE-0016 - Solar Academy). The research units LOCIE and FRESBE are members of the INES Solar Academy Research Center.

References

[1] IPCC, An ipcc special report on the impacts of global warming of 1.5° c above pre-industrial levels and related global greenhouse gas emission pathways, in the context of strengthening the global response to the threat of climate change, sustainable development, and efforts to eradicate poverty (2018).

[2] IRENA, Future of solar photovoltaic: Deployment, investment, technology, grid integration and socio-economic aspects, Report IRENA, A Global Energy Transformation 2019 (2019).

[3] REN21, Renewables 2019 global status report (2019).

[4] I. PVPS, Snapshot of global photovoltaic markets, Report IEA PVPS T1-33 2018 (2018).
[5] J. Von Appen, M. Braun, T. Stetz, K. Diwold, D. Geibel, Time in the sun: the challenge of high pv penetration in the german electric grid, IEEE Power and Energy magazine 11 (2013) 55–64.
[6] R. Perez, M. David, T. E. Hoff, M. Jamaly, S. Kivalov, J. Kleissl, P. Lauret, M. Perez, et al., Spatial and temporal variability of solar energy, Foundations and Trends® in Renewable Energy 1 (2016) 1–44.
[7] M. Obi, R. Bass, Trends and challenges of grid-connected photovoltaic systems–a review, Renewable and Sustainable Energy Reviews 58 (2016) 1082–1094.
[8] T. O. Olowu, A. Sundararajan, M. Moghaddami, A. I. Sarwat, Future challenges and mitigation methods for high photovoltaic penetration: A survey, Energies 11 (2018) 1782.
[9] P. Denholm, R. M. Margolis, Evaluating the limits of solar photovoltaics (pv) in electric power systems utilizing energy storage and other enabling technologies, Energy Policy 35 (2007) 4424–4433.
[10] O. Perpiñán, J. Marcos, E. Lorenzo, Electrical power fluctuations in a network of dc/ac inverters in a large pv plant: Relationship between correlation, distance and time scale, Solar Energy 88 (2013) 227–241.
[11] R. Luthander, J. Widén, J. Munkhammar, D. Lingfors, Self-consumption enhancement and peak shaving of residential photovoltaics using storage and curtailment, Energy 112 (2016) 221–231.
[12] R. Luthander, D. Lingfors, J. Widén, Large-scale integration of photovoltaic power in a distribution grid using power curtailment and energy storage, Solar Energy 155 (2017) 1319–1325.
[13] R. Luthander, J. Widén, D. Nilsson, J. Palm, Photovoltaic self-consumption in buildings: A review, Applied energy 142 (2015) 80–94.
[14] N. Sommerfeldt, H. Madani, Revisiting the techno-economic analysis process for building-mounted, grid-connected solar photovoltaic systems: Part one–review, Renewable and Sustainable Energy Reviews 74 (2017) 1379–1393.
[15] P. Dato, T. Durmaz, A. Pommeret, Smart grids and renewable electricity generation by households, Energy Economics 86 (2020) 104511.
[16] K. Fath, J. Stengel, W. Sprenger, H. R. Wilson, F. Schultmann, T. E. Kuhn, A method for predicting the economic potential of (building-integrated) photovoltaics in urban areas based on hourly radiance simulations, Solar Energy 116 (2015) 357–370.
[17] N. Lazard, Lazard's levelized cost of energy analysis–version 9.0, 2016.
[18] P. Redweik, C. Catita, M. Brito, Solar energy potential on roofs and facades in an urban landscape, Solar Energy 97 (2013) 332–341.
[19] S. Freitas, M. C. Brito, Solar façades for future cities, Renewable Energy Focus 31 (2019) 73–79.
[20] C.-M. Hsieh, Y.-A. Chen, H. Tan, P.-F. Lo, Potential for installing photovoltaic systems on vertical and horizontal building surfaces in urban areas, Solar Energy 93 (2013) 312–321.
[21] H. M. Lee, J. H. Yoon, S. C. Kim, U. C. Shin, Operational power performance of south-facing vertical bipv window system applied in office building, Solar Energy 145 (2017) 66–77.
[22] J. H. Kämpf, M. Montavon, J. Bunyesc, R. Bolliger, D. Robinson, Optimisation of buildings' solar irradiation availability, Solar Energy 84 (2010) 596–603.
[23] M. Bizjak, B. Žalik, N. Lukač, Evolutionary-driven search for solar building models using lidar data, Energy and buildings 92 (2015) 195–203.
[24] J. Widén, E. Wäckelgård, P. D. Lund, Options for improving the load matching capability of distributed photovoltaics: Methodology and application to high-latitude data, Solar Energy 83 (2009) 1953–1966.
[25] J. Natanian, O. Aleksandrowicz, T. Auer, A parametric approach to optimizing urban form, energy balance and environmental quality: The case of mediterranean districts, Applied Energy 254 (2019) 113637.
[26] C. Waibel, R. Evins, J. Carmeliet, Co-simulation and optimization of building geometry and multi-energy systems: Interdependencies in energy supply, energy demand and solar potentials, Applied Energy 242 (2019) 1661–1682.
[27] M. Brito, S. Freitas, S. Guimarães, C. Catita, P. Redweik, The importance of facades for the solar pv potential of a mediterranean city using lidar data, Renewable Energy 111 (2017) 85–94.
[28] S. Freitas, C. Reinhart, M. Brito, Minimizing storage needs for large scale photovoltaics in the urban environment, Solar Energy 159 (2018) 375–389.
[29] G. Desthieux, C. Carneiro, R. Camponovo, P. Ineichen, E. Morello, A. Boulmier, N. Abdennadher, S. Dervey, C. Ellert, Solar energy potential assessment on rooftops and facades in large built environments based on lidar data, image processing, and cloud computing. methodological background, application, and validation in geneva (solar cadaster), Frontiers in Built Environment 4 (2018) 14.
[30] M. Thebault, V. Clivillé, L. Berrah, G. Desthieux, Multicriteria roof sorting for the integration of photovoltaic systems in urban environments, Sustainable Cities and Society (2020) 102259.
[31] A. Walch, R. Castello, N. Mohajeri, J.-L. Scartezzini, Big data mining for the estimation of hourly rooftop photovoltaic potential and its uncertainty, Applied Energy 262 (2020) 114404.
[32] W. P. U. Wijeratne, R. J. Yang, E. Too, R. Wakefield, Design and development of distributed solar pv systems: Do the current tools work?, Sustainable cities and society 45 (2019) 553–578.

[33] A. Boccalatte, M. Fossa, C. Ménézo, Best arrangement of bipv surfaces for future nzeb districts while considering urban heat island effects and the reduction of reflected radiation from solar façades, Renewable Energy 160 (2020) 686–697.
[34] T. Durmaz, A. Pommeret, Levelized cost of consumed electricity, Economics of Energy & Environmental Policy 9 (2020).
[35] Photovoltaique.info - Connaitre les coûts et évaluer la rentabilité, 2020-10-08. URL: https://www.photovoltaique.info/fr/preparer-un-projet/quelles-demarches-realiser/choisir-son-modele-economique/
[36] Find minimum of constrained nonlinear multivariable function - MATLAB fmincon MathWorks, 2020-10-08. URL: https://fr.mathworks.com/help/optim/ug/fmincon.html.